

Research on Features for Diagnostics of Filtered Analog Circuits Based on LS-SVM

Bing Long^{1,3}, Shulin Tian¹, Qiang Miao^{2,3}, and Michael Pecht³

1-School of Automation Engineering, University of Electronic Science and Technology of China (UESTC), Chengdu 611731, China

2-School of Mechanical, Electronic and Industrial Engineering, UESTC, Chengdu 611731, China

3-Center for Advanced Life Cycle Engineering, University of Maryland, College Park, MD 20742, USA

Abstract—Feature selection techniques have become an apparent need for diagnostic methods such as a least squares support vector machine (LS-SVM). Most researchers use wavelet transform coefficients of the time-domain transient response data obtained from filtered analog circuits as features to train a LS-SVM classifier to diagnose faults. But wavelet coefficient features have certain disadvantages such as no physical meanings. Thus, in this paper, two new feature vectors with clearly defined meanings based on a time-domain response curve and a frequency response curve of a filter are proposed, respectively. In addition, a statistical property feature vector which represents global properties of the time-domain response curve or the frequency response curve is proposed. The results from the simulation data and real data for a biquad filter showed the following: (1) these proposed conventional time-domain and frequency features, which are already familiar to designers of filtered analog circuits, have good diagnostic accuracy—all above 91% for the example circuit; (2) the best accuracies using the proposed statistical property feature vector are 100% for time-domain simulation data, and for both real experiment data ; (3) the diagnostic accuracy using the proposed combined feature vector is more accurate than conventional feature vectors; (4) an LS-SVM can be used to diagnose faults in a real analog circuit that only has a few fault samples.

Keywords—*diagnostics; feature selection; feature vector; filtered analog circuits; least squares support vector machine (LS-SVM); time-domain features; frequency features*

I. INTRODUCTION

Fault diagnosis and fault location in analog and mixed signal circuits are important issues for design validation and prototype characterization [1]–[2]. In contrast to the well-developed automatic fault diagnosis methodologies for digital circuits, diagnostics of analog circuits is far less advanced due to poor fault models, components' tolerance, and nonlinearity issues of analog circuits [3]–[4]. Filtered analog circuits are widely used in the modern electronics industry for signal processing. Filtered analog circuits are also usually used as circuit under test (CUT) for diagnostics of analog circuits [3]–[10]. A biquad filter is used as a CUT in this paper.

Considering the trade-off between learning ability and generalizing ability by minimizing structure risk, support vector machines (SVMs) have been shown to be an effective

tool for the diagnostics of analog circuits [5]–[9]. Feature selection techniques have become an apparent need for diagnostic methods such as SVMs. Zhang et al. [5], and Liu et al. [6] directly used output voltage as features to train an SVM classifier for diagnostics of analog circuits. Cui and Wang [7] have used wavelet transform coefficients as features for diagnostics of a half-wave rectifier. Zuo et al. [8] and Long et al. [9] have developed the use of energy indicators of wavelet transform coefficients as features to train least squares SVMs (LS-SVMs) classifiers.

The aforementioned preprocessing methods can be classified into two categories: (1) no preprocessing at all [5]–[6]; and (2) preprocessing based on wavelet transform coefficients [7]–[9]. The SVM classifier without preprocessing often results in longer training time and less classification accuracy than a classifier with preprocessing techniques. The shortcomings of a preprocessing method based on wavelet transform include the following: (1) wavelet coefficient features have no physical meanings, which makes them difficult for designers of filters to understand; (2) selecting suitable coefficients among thousands of wavelet coefficients is difficult; (3) it is difficult to decide which kind of wavelet function and which level of wavelet decomposition should be used.

In addition, most researchers use time-domain features from an impulse response of filtered analog circuits to train SVMs. However, for filtered analog circuits, the frequency features, such as the center frequency and the maximum frequency response, are the key factors that indicate whether a filter system is working well.

LS-SVM modifies Vapnik's SVM formulation by adding a least squares term in the cost function, which significantly reduces the computational complexity [11]. LS-SVM is an appealing approach for diagnostics of filtered analog circuits. This paper will focus on feature selection for diagnostics of filtered analog circuits based on LS-SVM. First, two new feature vectors with clearly defined meaning based on time-domain response curves and frequency response curves are proposed in this paper. Then, since the two former feature vectors are relevant to the local properties of the response curves, a statistical property feature vector is proposed for representing the global properties of the time-domain response curve or the frequency response curve. The statistical vector is

This work was supported in part by National Natural Science Foundation of China under Grants 60673011 and 60934002, and in part by University of Electronic Science and Technology of China (UESTC) under Grants JX0756 and Y02018023601059.

composed of mean, stand deviation, skewness, kurtosis, and entropy of the response curve.

This paper is organized as follows: Section II presents the diagnostic procedure for filtered analog circuits based on LS-SVM and briefly reviews the principles of LS-SVM. Section III proposes two new feature vectors with clearly defined meanings and a statistical property feature vector based on time-domain and frequency response curves. Section IV shows the simulation and real experiment results for a biquad filter, and Section V presents our conclusions.

II. DIAGNOSTIC PROCEDURE AND LS-SVM

A. Diagnostic Procedure

A diagnostic procedure using an LS-SVM classifier for filtered analog circuits based on simulation experiments is shown in Fig. 1.

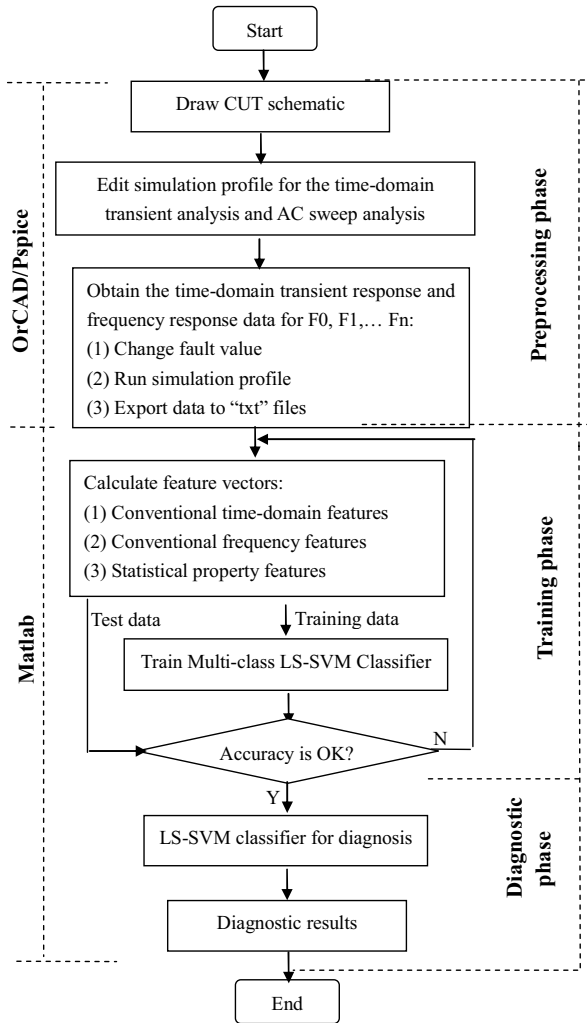


Fig. 1 Diagnostic procedure using an LS-SVM classifier based on simulation experiments.

The diagnostic procedure involves three phases, i.e., the preprocessing phase, the training phase, and the diagnostic phase. There are three steps involved in the preprocessing phase. First, the schematic of CUT is drawn and either the

Rbreak model or the Cbreak model is used for components with tolerance. Second, the parameters for the time-domain transient analysis and the Monte Carlo simulation analysis are set in a simulation profile. Third, according to each predefined fault class (including no fault F0, as seen in Table I, for example), the corresponding component is changed into a general component model and its parameter (for example, resistor value) is set to its fault value. Then the simulation profile is run to obtain the time-domain transient data or frequency response data, which are stored in .txt files. All three steps are implemented into electronic design automation software—OrCAD/Pspice [12].

In the training phase, the .txt files are imported into Matlab to calculate their feature vectors, which will be discussed in Section III; then, the data of each class are split into two parts: training data and test data. If the classification accuracy is better than the pre-defined accuracy, the classifier is ready to use for diagnosing faults in filtered analog circuits. Otherwise, a new feature set based on different criteria should be formed, and the classifier will be retrained with the new feature set. In the diagnostic phase, new data collected from the circuit can be inputted into the trained LS-SVM classifier for diagnostics.

The procedure for diagnostics of filtered analog circuits based on real data from an experiment is similar to that for simulation data except for the data used in the preprocessing phase. The simulation data will be replaced by the real data at the end of the preprocessing phase. The real data will act as the input for the training phase. This paper will illustrate the diagnostic procedures based on an LS-SVM classifier using both simulation data and real data from a biquad filter. To ensure the effectiveness, correctness, and repeatability of the simulation experiments, the LS-SVMlab toolbox [11] is used as a multi-class classifier.

B. LS-SVM

Consider a set of n data vectors

$$\{x_i, y_i\}, i = 1, \dots, n, y_i = \{-1, 1\} \quad (1)$$

where $x_i \in R^{m \times 1}$ is the i -th data (feature) vector that belongs to a binary class y_i . The classification problem is to find a set of weights $\omega \in R^{d \times 1}$ and a bias $b \in R$ term such that [11]:

$$y_i [\omega^T \cdot \phi(x_i) + b] \geq +1 - \xi_i \quad (2)$$

where $\phi: R^{m \times 1} \rightarrow R^{d \times 1}$ is a mapping that takes m dimensional input data into a d dimensional feature space; and ξ_i is the slack variable.

The objective of the SVM classification is to find a set of weights with the smallest norm that minimizes the sum of squared error terms [11]. That is,

$$\min_{\omega, \xi} J(\omega, \xi) = \omega^T \omega / 2 + \gamma \left(\sum_{i=1}^n \xi_i^2 \right) / 2 \quad (3)$$

where γ is a regularization parameter.

This is an optimization problem that can be solved by the Lagrangian function. The SVM classifier is as follows [11]:

$$f(z) = \text{sign}[w^T \phi(z) + b] = \text{sign}\left[\sum_{i=1}^n \alpha_i y_i \phi(x_i)^T \phi(z) + b\right] \quad (4)$$

where $z \in R^{m \times 1}$ is a new input vector to be classified.

C. Multi-class SVMs

Multi-class pattern recognition problems are typically solved by combining many binary classification SVMs. One-against-one SVM (OAOSVM) is suitable for practical use in diagnosis or classification [13]. OAOSVM for k -class classification constitutes $k(k-1)/2$ classifiers where each classifier is trained by data from two classes according to the previous LS-SVM algorithm. Then voting is used for future testing after all $k(k-1)/2$ classifiers are constructed, and the decision function is as follows [13]:

$$f_{ij}(z) = \text{sign}[w_{ij}^T \phi(z) + b_{ij}] \quad (5)$$

where w_{ij} and b_{ij} are the weight vector and bias of the i th and j th classes, respectively.

If $\text{sign}[w_{ij}^T \phi(z) + b_{ij}]$ says z is in the i th class, then one vote is given to the i th class. Otherwise the j th class gets one vote. Finally, z is predicted for the class with the largest vote.

III. FEATURES OF FILTERED ANALOG CIRCUITS

A. Conventional Time-Domain Features of Filtered Analog Circuits

A time-domain transient response curve of a filtered analog circuit is often obtained by a short impulse excitation, as shown in Fig. 2. Some properties of an impulse response curve, such as overshoot, rise time, delay time, settling time, and peak time, are familiar to designers of filters.

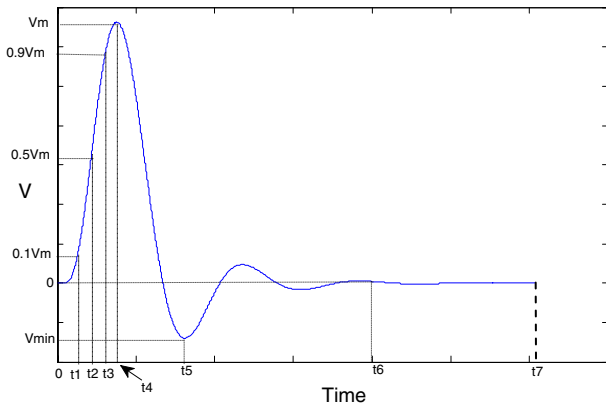


Fig. 2 Conventional time-domain features of an impulse response curve.

We use these properties to constitute a feature vector, which is called a conventional time-domain feature vector, and define it as follows:

$$FV_1 = [c_1, c_2, \dots, c_9] \quad (6)$$

where $c_1, c_2, c_3, c_4, c_5, c_6, c_7, c_8,$ and c_9 are the features that are relevant to overshoot, rise time, delay time, settling time,

maximum response value, time to reach the maximum response, minimum response value, time to reach the minimum response value, and fall time, respectively. These features are calculated as follows:

$$c_1 = V_m - V(t6) \quad (7)$$

$$c_2 = (t3 - t1)/t4 \quad (8)$$

$$c_3 = t2/t4 \quad (9)$$

$$c_4 = t6/t7 \quad (10)$$

$$c_5 = V_m \quad (11)$$

$$c_6 = t4 \quad (12)$$

$$c_7 = V \text{ min} \quad (13)$$

$$c_8 = t5 \quad (14)$$

$$c_9 = t5 - t4 \quad (15)$$

B. Conventional Frequency Features of Filtered Analog Circuits

A frequency response curve of a filtered analog circuit can be obtained by AC sweep. The frequency response curve for a low-pass filter is shown in Fig. 3. For designers of low-pass filters, maximum frequency response and cut frequency are key factors that reflect the performance of a filter. So we define a conventional frequency feature vector of a low-pass filter as follows:

$$FV_2 = [f_m, f_c, V_m, V_c] \quad (16)$$

where $f_m, f_c, V_m,$ and V_c are the features that are relevant to the frequency of the maximum frequency response point, upper cut frequency, the voltage of the maximum frequency response point, and the voltage of the upper cut frequency, respectively, as shown in Fig. 3.

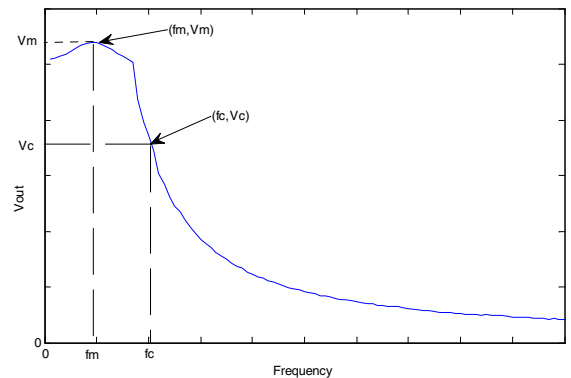


Fig. 3 Conventional frequency features of an AC sweep response curve for a low-pass filter

For high-pass filters, lower cut frequency rather than higher cut frequency should be used in the feature vector. For band-pass and band-stop filters, in addition to the maximum frequency response point, both the lower and the higher cut

frequency point can be used to constitute a feature vector.

C. Statistical Property Features of Filtered Analog Circuits

The conventional time-domain and frequency features are actually points on a time-domain impulse response curve or on a frequency response curve. They stand for the local properties of the curve. To determine the global properties of the curve, we propose using mean, standard deviation, skewness, kurtosis, and entropy to constitute a statistical feature vector for either a frequency response curve or a time-domain impulse response curve. That is,

$$FV_3 = [\mu, \sigma, s, k, e] \quad (17)$$

where μ , σ , s , k , e are mean, standard deviation, skewness, kurtosis, and entropy of the time-domain or frequency response data X respectively, and are defined below [4], [14], [15]:

$$\mu = E(X) \quad (18)$$

$$\sigma = \sqrt{\text{var}(X)} = \sqrt{E((X - m)^2)} \quad (19)$$

$$s = \frac{E(X - m)^3}{\sigma^3} \quad (20)$$

$$\text{kurt}(x) = E\{x^4\} - 3[E\{x^2\}]^2 \quad (21)$$

$$H(X) = -\sum_i P(X = a_i) \log P(X = a_i) \quad (22)$$

D. Combined Feature Vector of Filtered Analog Circuits

For time-domain features of filtered analog circuits, the combined feature vector is defined as

$$FV_4 = [FV_1, FV_3] \quad (23)$$

For frequency features of filtered analog circuits, the combined feature vector is defined as

$$FV_5 = [FV_2, FV_3] \quad (24)$$

where FV_1 , FV_2 , FV_3 are defined in (6), (16), (17), respectively

E. Feature Vector Normalization

We present two normalization methods to handle the effects of feature vectors' normalization: (1) all-normalized, and (2) partly-normalized. Assume that the original feature vector is

$$FV_0(i) = [f_1(i), f_2(i), \dots, f_j(i), \dots, f_m(i)] \quad (25)$$

where $i = 1, \dots, n$, $j = 1, \dots, m$, n is the number of samples, and m is the number of features for a sample.

The all-normalized method normalizes all features in the feature vector and is defined as follows:

$$FV_{-A}(i) = \left[\frac{f_1(i)}{\max_i(f_1(i))}, \frac{f_2(i)}{\max_i(f_2(i))}, \dots, \frac{f_j(i)}{\max_i(f_j(i))}, \dots, \frac{f_m(i)}{\max_i(f_m(i))} \right] \quad (26)$$

The partly-normalized method normalizes only some features. For FV_1 in (6), the partly normalized feature vector is defined as

$$FV_{1-P}(i) = \left[\begin{array}{c} c_1(i), c_2(i), c_3(i), c_4(i), c_5(i), c_6(i) / \max_i(c_6(i)), \\ c_7(i) / \max_i(\text{abs}(c_7(i))), c_8(i) / \max_i(c_8(i)), c_9(i) / \max_i(c_9(i)) \end{array} \right] \quad (27)$$

For FV_2 in (16), the partly-normalized feature vector is defined as

$$FV_{2-P}(i) = [f_m(i)/10^4, f_c(i)/10^4, V_m(i), V_c(i)] \quad (28)$$

For FV_3 in (17), the partly-normalized feature vector is defined as

$$FV_{3-P}(i) = [m(i), v(i), s(i), k(i) / \max_i(k(i)), e(i) / \max_i(e(i))] \quad (29)$$

IV. EXPERIMENT RESULTS

A. An Example Circuit

A four-op-amp biquad low-pass filter in [3], [4] is used as an example to show the diagnostic procedure based on LS-SVM using different feature vectors for simulation data and real data. A schematic of the filter is shown in Fig. 4, and detailed parameters of the filter are shown in Table I.

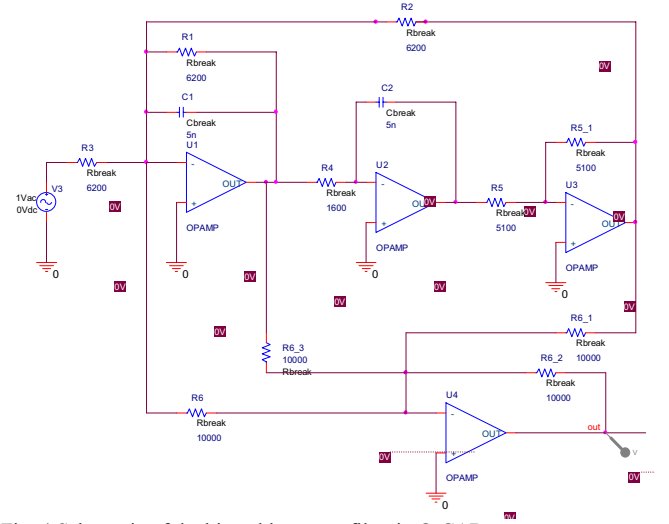


Fig. 4 Schematic of the biquad low-pass filter in OrCAD.

TABLE I
NOMINAL AND FAULT VALUES FOR THE BIQUAD FILTER

Fault ID	Fault Class	Nominal Value	Fault Value
F0	NF		
F1	C1 ↑	5nf	10nf
F2	C1 ↓	5nf	2.5nf
F3	C2 ↑	5nf	15nf
F4	C2 ↓	5nf	1.5nf
F5	R1 ↑	6200Ω	15000Ω
F6	R1 ↓	6200Ω	3000Ω
F7	R2 ↑	6200Ω	12000Ω
F8	R2 ↓	6200Ω	2000Ω
F9	R3 ↑	6200Ω	12000Ω
F10	R3 ↓	6200Ω	3300Ω
F11	R4 ↑	1600Ω	2500Ω
F12	R4 ↓	1600Ω	500Ω

B. Simulation Experiment Results Based on Time-Domain Features

According to equations (6), (17), (23), (26), (27), and (29), various kinds of time-domain feature vectors are used to train an LS-SVM classifier for diagnosing faults in the example circuit, Fig. 4. Using each feature vector as a test condition, for every predefined fault class (including F0, as shown in Table I) of the biquad filter, 100 samples from the Monte Carlo simulation are divided into two parts: the first 50 samples are used to train an LS-SVM classifier, and the other 50 samples are used to diagnose simulation faults of the filter. The total number of samples for the diagnostic phase is $50 \times 13 = 650$ due to there being 13 classes. The diagnostic procedure is shown in Fig. 1 and the diagnostic results for the test data are shown in Table II.

In Table II, ID stands for the serial number of each test condition, where test conditions 1–9 are for the biquad filter with 10% tolerance and test conditions 10–18 are for the filter with 5% tolerance. For the feature vectors in Table II, FV_{i_N} means that the feature vector FV_i in (6) is non-normalized; FV_{i_A} means that the feature vector FV_i is all-normalized by (26); FV_{i_P} mean that the feature vector FV_i is partly-normalized using (27). In Table II, the accuracy column is equal to the correct number of classified samples divided by the total number of test samples i.e. 650 in the example.

TABLE II
SIMULATION EXPERIMENT RESULTS BASED ON TIME-DOMAIN FEATURES

ID	Feature Vector	Accuracy
1	FV_{1_N}	99.85%
2	FV_{1_A}	94.46%
3	FV_{1_P}	99.08%
4	FV_{2_N}	97.54%
5	FV_{2_A}	90%
6	FV_{2_P}	100%
7	FV_{3_N}	100%
8	FV_{3_A}	97.85%
9	FV_{3_P}	99.23%
10	FV_{1_N}	100%
11	FV_{1_A}	95.85%
12	FV_{1_P}	99.38%
13	FV_{2_N}	99.38%
14	FV_{2_A}	94%
15	FV_{2_P}	99.85%
16	FV_{3_N}	100%
17	FV_{3_A}	100%
18	FV_{3_P}	100%

The results from Table II can be summarized as follows:

(1) For the proposed conventional time-domain feature vectors (ID: 1-3, 10-12), the diagnostic accuracies were good, all being above 94%. The best accuracy was 99.85% for the filter with 10% tolerance, and it was 100% for the filter with 5% tolerance.

(2) For the proposed statistical property feature vectors (ID: 4–6, 13–15), the diagnostic accuracy for test data was also good. The best accuracy was 100% for the filter with 10% tolerance and 99.85% for the filter with 5% tolerance.

(3) The diagnostic accuracies using the combined feature

vectors (ID: 7–9, 16–18) were better than using conventional time-domain feature vectors (ID: 1-3, 10-12). For the filter with 10% tolerance, 7-9 are better than 1-3 correspondingly. For the filter with 5% tolerance, there was one instance of 100% accuracy for the conventional feature vector (ID: 10) while all the three combined vectors were 100% (ID: 16–18).

C. Simulation Experiment Results Based on Frequency Features

According to equations (16), (17), (24), (26), (28), and (29), various kinds of feature vectors are used to train the LS-SVM classifier for diagnosing faults in the example circuits. Using a method similar to the one presented in part B in this section to produce the training data and test data, the diagnostic results for the test data are shown in Table III.

For ID in Table III, test conditions 1–9 are for the biquad filter with 10% tolerance, and the test conditions 10–18 are for the filter with 5% tolerance.

TABLE III
SIMULATION EXPERIMENT RESULTS BASED ON FREQUENCY FEATURES

ID	Feature Vector	Accuracy
1	FV_{2_N}	90.31%
2	FV_{2_A}	33.54%
3	FV_{2_P}	91.23%
4	FV_{2_N}	89.08%
5	FV_{2_A}	90.77%
6	FV_{2_P}	99.38%
7	FV_{3_N}	92%
8	FV_{3_A}	98.62%
9	FV_{3_P}	99.85%
10	FV_{2_N}	91.69%
11	FV_{2_A}	32%
12	FV_{2_P}	91.85%
13	FV_{3_N}	91.69%
14	FV_{3_A}	88.62%
15	FV_{3_P}	99.38%
16	FV_{2_N}	91.23%
17	FV_{2_A}	98.77%
18	FV_{2_P}	99.85%

The results from Table III can be summarized as follows:

(1) For the proposed conventional frequency feature vector (ID: 1–3, 10–12), normalization has a significant impact on the accuracy. The accuracies of the all-normalized vectors (i.e., 2, 5, 8, 11, 14, and 17) were lower than non-normalized or partial-normalized. The worst accuracies (ID: 2, and 11) are only one-third of the accuracies of the same combination of feature vector.

(2) For the proposed statistical property feature vector (ID: 4–6, 13–15), the best accuracies were both 99.38% for the filter with 10% and 5% tolerance and were both obtained using a partly-normalized vector.

(3) The diagnostic accuracies using the combined feature vectors (ID: 7–9, 16–18) were better than using conventional frequency feature vectors (ID: 1-3, 10-12). For the filter with 10% tolerance, the best accuracy for the conventional feature vectors is 91.23% (ID: 3), while the best accuracy for the combined vectors is 99.85% (ID: 9). For the filter with 5%

tolerance, the best accuracy for the conventional feature vectors is 91.85% (ID: 12), while the best accuracy for the combined vectors is 99.85% (ID: 18).

D. Real Experiment Results

To illustrate the procedure for diagnostics of filtered analog circuits based on real experiment data, we also conducted two real experiments: for a) AC sweep frequency response data, and b) time-domain transient data. The setup of the experiments for the biquad filter is shown in Fig. 5. The schematic of the biquad filter is shown in Fig. 4 and the nominal and fault values for the components are shown in Table II. It is time-consuming to collect many fault samples for each fault class to train an LS-SVM classifier because we will have to replace a component or adjust a parameter's value manually. Therefore, we first collected as many points as possible for one fault class, and then the fault data was divided into several samples for the same fault class. Using this method, we obtained 10 samples for each fault class from a time-domain response experiment and 4 samples for each fault class from a frequency response experiment.

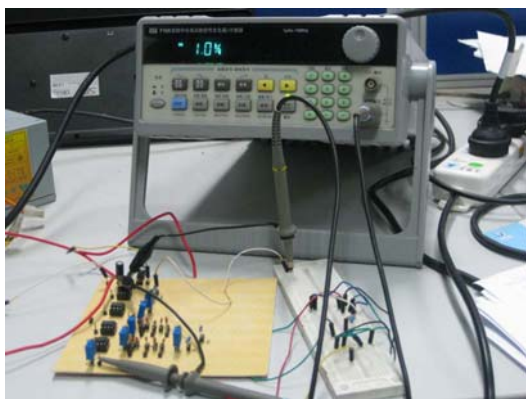


Fig. 5 Setup of real experiments for the biquad filter.

For the time-domain transient experiment, a time-domain transient response curve of the fault-free (i.e., F0) biquad filter is shown in Fig. 6. There are 500 points in the curve, and these data can be divided into 10 samples. So there are 50 data points for one sample. Due to the limited number of samples, all 10 samples for each class are used as both the training data and the test data. The total number of samples for the diagnostic phase is $10 \times 13 = 130$ due to there being 13 classes. Feature vectors similar to those mentioned in part B of this section were calculated based on the test data. The diagnostic results are shown in Table IV where there are no FV_{1_A} and FV_{4_A} because some features in FV_1 are zeros. In Table IV, Time column includes the training and test time by the LS-SVM classifier only

The results from Table IV show the following: (1) although we have only a few experimental samples we can use an LS-SVM for diagnostics of filtered analog circuits. Moreover, (2) the diagnostic accuracy is very good: the accuracies for the LS-SVM classifiers using both the statistical property feature vector FV_3 and the combined feature vector FV_4 can reach 100% while the best accuracy using the conventional time feature vector was 97.69%. (3) The diagnostic time is less

than 10 seconds if using suitable feature vectors such as FV_{3_P}, FV_{4_P} .

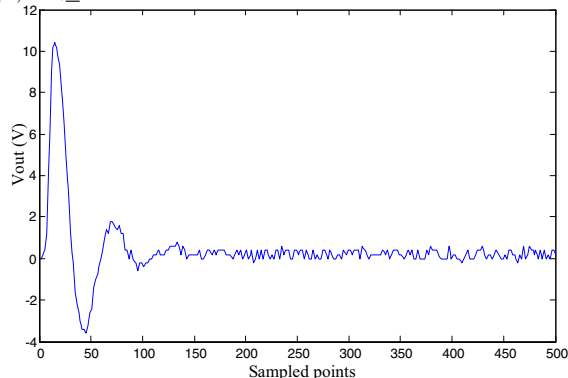


Fig. 6 A time-domain transient response curve of the fault-free biquad filter.

TABLE IV
REAL EXPERIMENT RESULTS BASED ON TIME-DOMAIN FEATURES

ID	Feature Vector	Accuracy	Time(s)
1	FV_{1_N}	97.69%	8.97
2	FV_{1_P}	86.15%	19.59
3	FV_{3_A}	84.62%	18.47
4	FV_{3_N}	66.92%	34.35
5	FV_{3_P}	100 %	6.94
6	FV_{4_N}	93.08%	17.25
7	FV_{4_P}	100%	9.16

A frequency response curve of the fault-free biquad filter is shown in Fig. 7. There are 100 points in the curve, and these data can be divided into 4 samples. So there are 25 data points for one sample. Due to the limited number of samples, all 4 samples for each class are used as both the training data and test data. The total samples for the diagnostic phase are $4 \times 13 = 52$ due to there being 13 classes. Feature vectors similar to those mentioned in part C of this section were calculated based on the test data. The diagnostic results are shown in Table V.

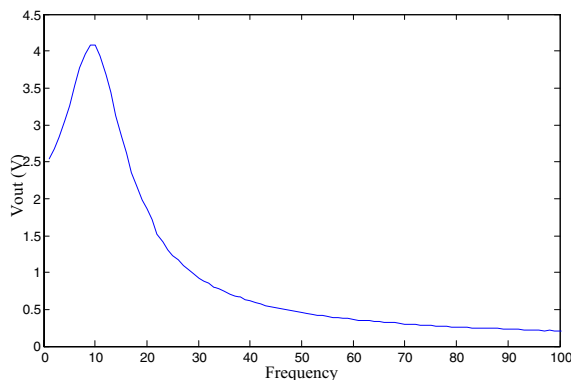


Fig. 7 A frequency response curve of the fault-free biquad filter.

The results from Table V show: (1) the best accuracy using the conventional frequency feature vector (ID: 1) is 98.08%; (2) the accuracies using both the statistical property feature vector and the combined feature vector (ID: 6, and 7) can reach 100%; (3) this filter was originally determined to be a **high-pass** filter in [3], [4], but it is actually a **low-pass** filter that can be confirmed from the real frequency response curve in Fig. 7. This shows frequency features are more important

than time-domain features for filtered analog circuits. (4) The diagnostic time is also less than 10 seconds if using suitable feature vectors such as FV_{3_P}, FV_{5_P} .

TABLE V
REAL EXPERIMENT RESULTS BASED ON FREQUENCY FEATURES

ID	Feature Vector	Accuracy	Time(s)
1	FV_{2_N}	98.08%	4.18
2	FV_{2_A}	63.46%	15.47
3	FV_{2_P}	92.31%	5.47
4	FV_{3_N}	92.31%	5.41
5	FV_{3_A}	84.62%	12.29
6	FV_{3_P}	100%	3.76
7	FV_{5_N}	100%	5.83
8	FV_{5_A}	92.31%	12.35
9	FV_{5_P}	100%	4.26

V. CONCLUSIONS

Through the results from the simulation experiment and the real experiment for diagnostics of a biquad filter, we can draw the following conclusions:

(1) The diagnostic accuracy using proposed conventional time-domain feature vector is over 97% for both the simulation data and the real data from the biquad filter.

(2) The proposed conventional frequency features are key factors that reflect the performance of filtered analog circuits. Using the feature vector, the diagnostic accuracy is over 91% for simulation data and over 98% for the real data of the biquad filter.

(3) The diagnostic accuracy using the proposed statistical property feature vector is good. For time-domain experiments, the best accuracy is 100% for both simulation data and real data of the biquad filter. For frequency response experiments, the best accuracy is 99.38% for the simulation data and is 100% for the real data of the biquad filter.

(4) The diagnostic accuracy using the proposed combined feature vector has better accuracy than using conventional feature vectors. Using the combined vector, the best accuracies are 100% for nearly all the simulation and real data of the biquad filter except for the simulation data of a frequency response experiment.

(5) LS-SVM can be used to diagnose faults in a real filtered analog circuit that only has a few fault samples. We can divide a fault sample into several samples if there are enough data in one sample. The diagnostic accuracy can reach 100% if suitable feature vectors are used, though there are only 10 samples for each class of the time-domain experiment and only 4 samples for each class of frequency response experiment.

ACKNOWLEDGMENT

The authors would like to thank Mark Zimmerman for his help in copyediting and to thank anonymous reviewers' valuable comments on this paper.

REFERENCES

- [1] S. J. S. Mahdavi, K. Mohammadi, Evolutionary derivation of optimal test sets for neural network based analog and mixed signal circuits fault diagnosis approach, *Microelectronics Reliability* 49 (2009) 199–208
- [2] R. Voorakaranam, S. S. Akbay, Signature testing of analog and rf circuits: algorithms and methodology, *IEEE Transaction on Circuits and Systems-I: Regular Papers*, vol. 54, no.5, pp.1018-1031, 2007.
- [3] M. Aminian, F. Aminian, A modular fault-diagnostic system for analog electronic circuits using neural networks with wavelet transform as a preprocessor, *IEEE Transaction Instrumentation and Measurement*, vol. 56, no.5, pp.1546-1554, 2007
- [4] L.F Yuan, Y.G. He, J.Y. Huang, Y.C. Sun, A new neural-network-based fault diagnosis approach for analog circuits by using kurtosis and entropy as a preprocessor, *IEEE Transaction Instrumentation and Measurement*, vol. 59, no.3, pp.586-595, 2010
- [5] Y. Zhang, X.Y. Wei, H.F. Jiang, One-class classifier based on SBT for analog circuit fault diagnosis, *Measurement* 41 (2008) 371–380.
- [6] Y.H. Liu, Y.Y Yang, L. Huang, Fault diagnosis of analog circuit based on support vector machines, *Proceedings of ICCTA2009*, pp. 40-43, 2009
- [7] J. Cui and Y.R. Wang, A novel approach of analog circuit fault diagnosis using support vector machines classifier, *Measurement* 44 (2011)-289
- [8] L. Zuo, L.G. Hou, W. Zhang, W.C.Wu. Applying wavelet support vector machine to analog circuit fault diagnosis, *2010 Second International Workshop on Education Technology and Computer Science*, pp. 75-78, 2010
- [9] B. Long, S.L. Tian, H.J. Wang. Least squares support vector machine based analog-circuit fault diagnosis using wavelet transform as preprocessor, *ICCCAS 2008*: 1026-1029
- [10] A. Williams and F. Taylor, *Electronic Filter Design Handbook* (Fourth Edition), New York: McGraw-Hill, 2006.
- [11] J.A.K. Suykens, T. Van Gestel, J. De Brabanter, B. De Moor, J. Vandewalle, *Least Squares Support Vector Machines*, World Scientific, Singapore, 2002
- [12] John Keown, *OrCAD PSpice and Circuit Analysis (4th Edition)*, Prentice Hall, 2000
- [13] C-W Hsu, C-J Lin, A comparison of methods for multi-class support vector machines, *IEEE Transaction on Neural Network*, vol. 13, no.2, pp. 415-425, 2002
- [14] A. Papoulis, *Probability, Random Variables, and Stochastic Processes*, 3rd ed. New York: McGraw-Hill, 1991
- [15] A. Tafazzoli, N. M. Steiger, J. R. Wilson. N-skart: a non sequential skewness- and auto regression-adjusted batch-means procedure for simulation analysis, *IEEE Transaction on Automatic Control*, Vol. 56, no. 2, pp. 254-264, February 2011